Nucleoside–Lipid-Based Nanoparticles for Cisplatin Delivery

Salim Khiati,[†,‡] Delphine Luvino,[§] Khalid Oumzil,[†,‡] Bruno Chauffert,[⊥] Michel Camplo,[§] and Philippe Barthélémy[†,‡,*]

[†]INSERM U869, Bordeaux F-33076, France, [‡]Université de Bordeaux, Bordeaux F-33076, France, [§]CINaM, Université de la méditerranée, 13288 Marseille cedex 9, France, and [⊥]CHU Amiens-Picardie, 80054 Amiens Cedex, France

ABSTRACT The use of delivery vehicles to selectively transport anticancer agents to tumors is very attractive to address both toxicity and efficacy issues. We report a novel approach based on hybrid nucleoside–lipids allowing the efficient encapsulation and delivery of cisplatin. We demonstrate that the nucleoside polar heads guide the self-assembly of the aggregates into highly loaded and stable nanoparticles. The nanoparticles, which are efficient vehicles for the delivery of cisplatin into different sensitive and resistant cancer cell lines, can overcome the disadvantages and limitations of drug delivery systems previously reported.

KEYWORDS: nanoparticles · cisplatin · drug delivery · nucleoside–lipids · cancer

Among the anticancer drugs, cisplatin is one of the most widely used and effective cytotoxic agents in the treatment of tumors and malignancies. It is currently used in combination with other drugs, as first line treatment against cancers of the lung, head and neck, ovaries, esophagus, stomach, colon, bladder, testis, cervix, and uterus and as second line chemotherapy against most other advanced cancers such as cancers of the pancreas, liver, kidney, prostate, as well as against glioblastomas and metastatic melanomas.[1−3] Nevertheless, the emergence of intrinsic and acquired resistance still limits the clinical use of this drug.[4] Severe side effects, including acute nephrotoxicity and chronic neurotoxicity, limit its optimum use for a large number of patients.[5,6] Hence, the development of new efficient drug delivery systems (DDS)[7−10] which would provide a higher accumulation of cisplatin in cancer cells has been under investigation by different academic and industrial groups.[11] Some of them have been evaluated on humans in clinical trials.[12] It was shown almost 10 years ago by Burger *et al.*[13] that lipid-coated nanoparticles of cisplatin could enhance the antitumor efficacy. Since then, different generations of DDS dedicated to the vectorization of cisplatin have been reported, including polymeric micelles,[14−17] liposomes,[18] and cisplatin prodrug nanoparticles.[19−21] However, several physicochemical drawbacks, such as, for example, drug loading or stability in physiological conditions, still prohibit the clinical use of these DDS.

Here we demonstrate that nucleoside–lipids[22,23] can be used to control the precipitation of cisplatin to the extent that the nucleoside polar heads guide the self-assembly of the aggregates into highly loaded and stable nanoparticles. We show that nucleoside–lipid-based nanoparticles, which are efficient vehicles for the delivery of cisplatin into different cancer cell lines, can overcome the limitations of ciplatin NPs previously reported.

RESULTS AND DISCUSSION

Design, Preparation, and Characterization of NPs. The unique supramolecular capabilities of the hybrid molecules derived from nucleotides and lipids and their nontoxic properties render them ideal candidates for encapsulating platinum drugs. In this work, a simple encapsulation procedure was used to address the physicochemical properties such as stability and drug loading, which limit the clinical use of most DDS. Our method involves two steps: (i) the encapsulation of the cisplatin nanoprecipitate *via* an anionic nucleotide–lipid,[24] diC_{16}-3′-dT (thymidine 3′-(1,2-dipalmitoyl-*sn*-glycero-3-phosphate)); and (ii) the stabilization of the resulting anionic nanoparticles using a cationic nucleoside–lipid DOTAU[25] (2′,3′-dioleyl-5′-deoxy-5′-trimethylammoniumuridine) (Figure 1A).

In a first attempt to prepare highly loaded stable nanoparticles of cisplatin, we adapted the freeze–thaw multicycle procedure previously reported by Burger *et al.*[26] to colloidal suspensions of diC_{16}-3′-dT/DOPC (1/1) and cisplatin (5 mM). As expected, thanks to the electrostatic interactions between negatively charged phospholipids and positively charged aqua

* Address correspondence to philippe.barthelemy@inserm.fr.

Received for review June 21, 2011 and accepted September 30, 2011.

Published online September 30, 2011 10.1021/nn202291k

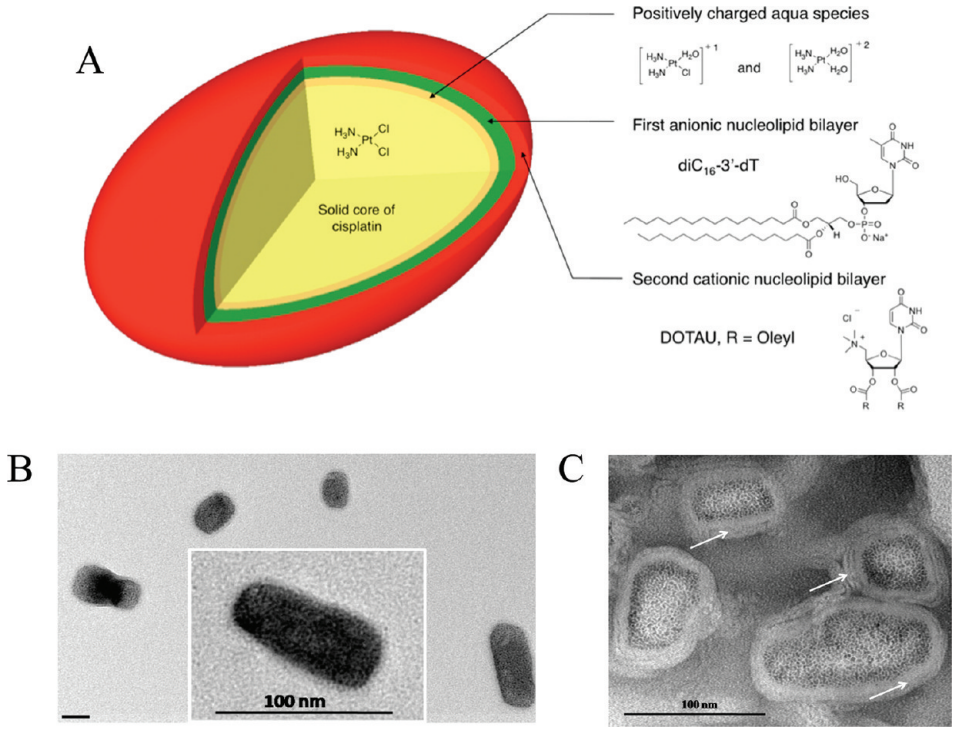

Figure 1. (A) Nanoparticle schematic drawing, chemical structures of an anionic nucleotide−lipid, the thymidine 3′-(1,2-dipalmitoyl-*sn*-glycero-3-phosphate) (diC$_{16}$-3′-dT), and a cationic nucleoside−lipid DOTAU (2′,3′-dioleyl-5′-deoxy-5′-trimethylammoniumuridine) used in this study. (B) TEM image of diC$_{16}$-3′-dT/DOPC cisplatin-loaded anionic nanoparticles after uranyl acetate negative staining; scale bar = 50 nm. The TEM image inset shows a magnification of a negative nanoparticle NP−. (C) TEM images of cisplatin-loaded NP+ after uranyl acetate negative staining. The arrows indicate the multilayer systems.

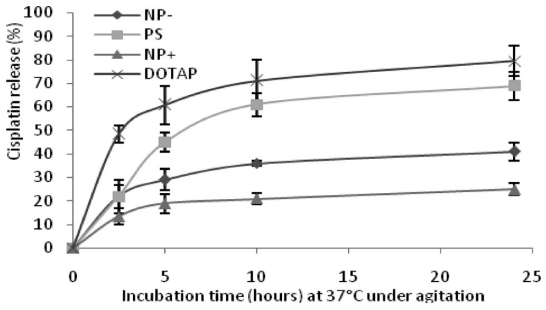

Figure 2. Cisplatin release of nanoparticles after water incubation at 37 °C under 300 rpm agitation. Anionic nanoparticles: diC$_{16}$-3′-dT/DOPC (NP−) and DOPS/DOPC (PS). Cationic nanoparticles: DOTAU (NP+) and DOTAP (DOTAP).

species[27] of cisplatin, this procedure provided nanoparticles of cisplatin similar to the ones previously reported with DOPS/DOPC (1/1) formulations.[26,28] In accordance with dynamic light scattering (DLS) data (Figure S1 in the Supporting Information), transmission electron microscopy (TEM) images show oblong monodisperse objects of 50−100 nm long with a solid core of platinum (Figure 1B). Zeta-potential measurements show negative values of −49 ± 6.2 mV for both diC$_{16}$-3′-dT/DOPC (NP−) and DOPS/DOPC (PS) nanoparticles, indicating that negative lipids (diC$_{16}$-3′-dT and/or DOPS) wrap the solid core (Figure S2). Next, to evaluate the stability of both formulations, NP− and PS nanoparticles were incubated at 37 °C either in the absence or in the presence of serum. In the absence of serum (Figure 2), the NP− is more stable than PS, showing a release of 35 and 70% after 24 h, respectively. These first results indicate that the nucleolipid layer stabilizes the nanoparticle structure, likely due to additional favorable interactions provided by the diC$_{16}$-3′-dT nucleotide−lipid at the solid core surface. FTIR spectra performed at room temperature with NP− nanoparticles exhibit a decrease of the thymine C═O stretching vibrations initially observed with pure diC$_{16}$-3′-dT at 1692 cm^{-1}. These observations indicate that nucleoside-based phospholipids are involved in new interactions within the nanoparticles (Figure S3). However, the presence of serum in similar conditions induced a strong destabilization of both systems, resulting in a total release of cisplatin after only 2 h of incubation (Figure S5). These results show that both types of negatively charged nanoparticles cannot be used for *in vivo* conditions.

Since the NPs have to reach the target tumor cells to be efficient, the stability in physiological conditions is a critical issue. To overcome the stability problem, we hypothesize that the addition of a second layer of nucleolipids at the surface of the NPs would enhance their stability. The rationale behind this approach is to take advantage of both electrostatic and base−base interactions between nucleolipids at the nanoparticles'

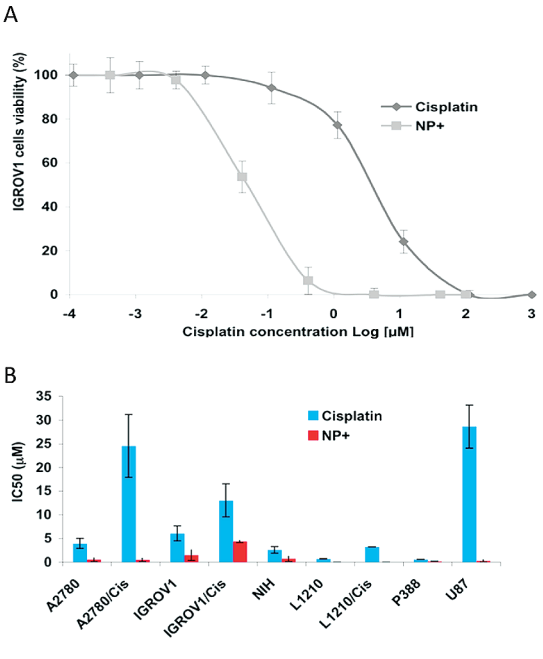

Figure 3. (A) Cytotoxic effect on IGROV-1 cancer cell line of free cisplatin compared to the cisplatin-loaded nanoparticles (NP+). (B) Comparison of cytotoxicities of the cisplatin-loaded NP+ nanoparticles compared to conventional free cisplatin in various human carcinoma cell lines. The IC_{50} values (μM) reported were determined on the A2780, A2780/cisplatin-resistant, IGROV-1, IGROV-1/cisplatin-resistant, L1210, L1210−1/cisplatin-resistant, NIH:OVCAR-cell lines and P388. Nanoparticles are much more cytotoxic than free conventional cisplatin on all of the cell lines tested. The IC_{50} ratios are for cell lines from left to right, 14 (A2780), 107 (A2780/cis), 12 (IGROV1), 3 (IGROV-1/cis), 8 (NIH), 3 (L1210), 130 (L1210/cis), 3 (P388), and 136 (U87). Cytotoxicity was determined using an MTT assay.

surface. Hence, the negative NP− nanoparticles were incubated in the presence of a positively charged nucleolipid DOTAU.[25] This additional step provided positive nano-objects (zeta-potential of NP+ = +48.4 ± 7.6 mV (Figure S2)) of around 100 nm in diameter (Figure S1), indicating that a second positive bilayer encapsulates the first one. The presence of a second nucleolipid bilayer at the NP surface was confirmed by XPS analysis (Figure S4). In this experiment, a value of 2.56% for nitrogen corresponding to the ammonium group of DOTAU was measured, whereas no phosphate (diC_{16}-3′-dT) was detected in the external layer.

The multilayer system was observed on TEM images (Figure 1C). A comparative study of NP stabilities measured at 37 °C in water (absence of serum) is presented in Figure 2. Note, that NP+ featuring a multilayer system composed of diC_{16}-3′-dT and DOTAU exhibited an increased stability compared to previously reported nanoparticles (PS) and negative NP−. With less than 25% of release for NP+ and after 24 h of incubation in the absence of serum at 37 °C, NP+ nanoparticles are much more stable than the PS-based NPs previously reported (70% of release after 24 h). Noteworthy, in a control experiment, the NP− nanoparticles were incubated in the presence of DOTAP, which overall can be viewed as a non-nucleolipid cationic analogue of DOTAU. Despite the presence of cationic lipid allowing electrostatic interactions with the negative charge of the NP− surface, this formulation was poorly stable (80% of release after 24 h), demonstrating that nucleobases are playing a crucial role in the stabilization of cisplatin-loaded NPs (Figure 2). Importantly, in the presence of serum at 37 °C, the half-life observed for NP+ was higher than 2 h, whereas a total release of cisplatin is observed after only 1 h for both negative PS and NP− nanoparticles, indicating that only NP+ can be used for delivery applications (Figure S5). The evaluation of the drug loaded into NPs was performed after determination of the amount of encapsulated cisplatin by optical ICP-AES analysis. The NP+ formulations feature very high drug loading (DL) capacities (DL = 60.5%, cisplatin weight/total weight).

Antitumoral Activities. In order to evaluate the potential of our technology, we have determined the concentrations of novel cisplatin nanoparticles to obtain a 50% inhibition of proliferation (IC_{50}) against a panel of tumor cell lines. The cell lines chosen for this study are the following: (a) A2780 and A2780/cisplatin-resistant cell lines, (b) IGROV-1 and IGROV-1/cisplatin-resistant cell lines, (c) L1210 and L1210/cisplatin-resistant cell lines, (d) NIH:OVCAR-3 cell line, (e) P388, and (f) U87 cell line. For example, Figure 3A shows the growth inhibition of human ovarian IGROV-1 tumor cells induced by cisplatin-loaded nanoparticles prepared from nucleoside-based lipids. The lipid-containing formulation exhibits increased cytotoxic activity, with an IC_{50} value more than 2 orders of magnitude lower than that of free cisplatin. In addition, nanoparticles show unprecedented *in vitro* toxicity up to 130-fold higher than that of the free drug. For example, as shown on Figure 3B, nanoparticles are 14-fold and 8-fold more toxic than free cisplatin in the case of sensitive cell lines A2780 and NIH, respectively.

Importantly, the nanoparticles are much more effective than the free drug against cisplatin-resistant cell lines (IC_{50} ratios of 107 and 130 for A2780/cisplatin and L1210/cisplatin resistant, respectively) (Figure 3B). In the case of the IGROV-1 cisplatin-resitant cell line, a moderated IC_{50} ratio of 3 was observed. In addition, cationic NPs are also highly efficient against glioblastoma cancer cells (brain tumor). For these cells, cationic NPs are 136-fold more active than free cisplatin (Figure 3B).

The antitumoral activities of nucleolipid-based NPs (NP+ and NP−) were also compared to the efficacy of previous PS-based nanoparticles (Figure S6). NP+ and NP− were more cytotoxic for IGROV-1 cells compared to PS nanoparticles, whereas for SKOV-3 cells, only NP+ nanoparticles were more cytotoxic than PS nanoparticles. Note that the nucleolipids without cisplatin do not

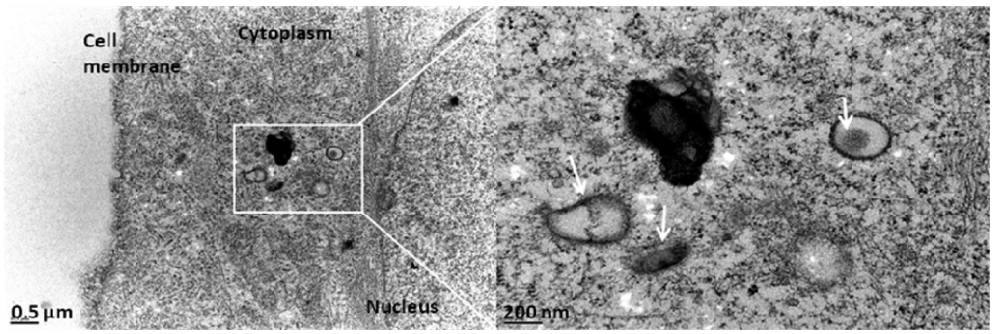

Figure 4. TEM imaging of SKOV-3 cell after 2 h incubation in the presence of NP+. The arrows show the nanoparticles in the endosomes.

show any toxicity *in vitro* at a concentration 10 times higher than the amount of lipids in NP+ (no toxicity was observed until 500 mM). *In vivo* injection of both nucleolipids at 4 mg/kg in mouse does not exhibit any toxicity (Table S1). Likewise, the maximum tolerated doses (MTD) observed *in vivo* for the cisplatin-loaded NPs are enhanced with concentrations in cisplatin higher than 9 mg/kg (MTD of free cisplatin is 5 mg/kg), indicating that NPs can be intravenously injected at higher concentrations in cisplatin than the free drug (Figure S7).

Next, to determine whether the cytotoxicity observed was due to either the NP objects intrinsically or to the drug itself, we exposed the SKOV-3 and IGROV-1 cell lines to NPs+ resulting from the encapsulation of either cis or trans platinum drugs using the same protocol. Transplatin, an isomer of cisplatin, is known to be poorly active against cancer cells.[29] After incubating ovarian cancer cells (IGROV-1) for 2 h in the presence of NPs, DNA analysis (Figure S8A) and MTT assays show a lower efficiency of transplatin NP compared to cisplatin NP (Figure S8B). IC_{50} values for cisplatin−NP+ compared to transplatin−NP+ (0.5 and 10 μM, respectively, Figure S8B) demonstrate that the highest cytotoxicity observed for cisplatin−NP+ is due to the encapsulated drug and not to the nano-objects intrinsically.

A major issue in chemotherapy is the resistance appearing after treatment with an anticancer drug.[30] Different mechanisms have been reported, including the modification of uptake and efflux of cisplatin, inactivation of the drug by sulfur-containing molecules (glutathione), alterations in the expression of oncogenes and tumor suppressor genes (such as p53), inhibition of apoptosis, *etc*.[31,32] To evaluate whether the NP+ nanoparticles were able to overcome the resistant phenomena, the growth of IGROV-1 (sensitive) and SKOV-3 (resistant, absence of p53 expression) cells was followed for one month after one treatment with 5 mM of equivalent cisplatin using the different formulations such as free cisplatin, NP−, PS, and NP+ (Figures S9 and S10). Interestingly, only the NP+ nanoparticles were able to avoid a total regrowth of both tumor cell lines after one month, whereas a regrowth was observed for all of the other formulations. A regrowth was observed after 5 and 12 days for free cisplatin and negative NPs (NP− and PS), respectively, in the case of IGROV-1. SKOV-3 cells regrow after 20 days for negative NPs (NP− and PS). These results suggest that only NP+ can deliver a sufficient amount of active drug into cells to prohibit tumor regrowth.

To explain these different effects, the cellular uptake of the NP+ was first investigated using confocal microscopy (Figure S11) and TEM (Figure 4). The confocal images indicated that NP+ nanoparticles labeled with DOPE-Rhodamine were uptaken by the cells. Electronic microscopy images showed that NP+ nanoparticles are located in the endosomes (Figure 4 right, arrows) The amount of cisplatin internalized into IGROV-1 and SKOV-3 cells incubated in the presence of different formulations was measured by ICP optical emission spectrometry (Figures S12 and S13). As expected, the amount of cisplatin internalized into IGROV-1 was 20 times higher for NP+ than for free cisplatin, whereas the amount internalized for both NP− and PS was only 3−5 times higher compared to the free drug. Likewise, in the case of SKOV-3, NP+ nanoparticles were the most effective with an amount of drug internalized 30 times higher than free cisplatin.

The construction of nanoparticles *via* the "layer-by-layer" approach reported in this contribution allows the insertion of a second lipophile anticancer drug in these layers, which act as hydrophobic reservoirs. Hence, to validate the multicompartment feature inherent to NP+, lipophilic fluorescent probes (fluorescein-DOPE and rhodamine-DOPE) were inserted in the formulations as labeling agents. For FACS and microscopy studies, the following three different systems were prepared: (i) NP_1+, diC_{16}-3′-dT first layer labeled with fluorescein-DOPE; (ii) NP_2+, DOTAU second layer labeled with rhodamine-DOPE; and (iii) NP_3+, both layers labeled with fluorescein-DOPE and rhodamine-DOPE, respectively. FACS analysis of SKOV-3 cells incubated with (i) NP_1+ (Figure S14B), (ii) NP_2+ (Figure S14C), and (iii) NP_3+ (Figure S14D) indicate that nanoparticles are maintained intact after cellular internalization. Interestingly,

fluorescence microscopy imaging of SKOV-3 treated with NP_3+ showed the superposition of green fluorescence (fluorescein) and red fluorescence (rhodamine) into the cells (Figure S15), confirming the internalization of NP_3+ as a labeled multilayer system.

CONCLUSION

Overall, our results demonstrate that lipids featuring molecular recognition principles afford an original and powerful approach to address the cisplatin delivery issue. The nucleolipid-based nanoparticles can overcome most of the disadvantages or limitation associated with previously reported encapsulation techniques, including high drug loading and stability. Furthermore, these new NPs appear as ideal candidates for their use as a vehicle for cisplatin delivery as witnessed by the increased antitumor activities observed on cisplatin-sensitive and -resistant cell lines. In light of these results, nanoparticle supramolecular systems based on biomimetic interactions should contribute to the emergence of major routes for the design and development of efficient nontoxic drug delivery systems.

METHODS

Preparation of Cisplatin Anionic Nanoparticles. Cisplatin diluted in deionized (DI) water (5 mM) was incubated at room temperature for 48 h under stirring. Dry lipid film composed of equimolar amounts of DOPC and diC_{16}-3′-dT (1.2 mmol) was incubated overnight at room temperature with 1.2 mL of the 5 mM aqueous solution of cisplatin. The mixture was subjected to 10 cycles of freeze−thaw using ethanol/dry ice (−70 °C) and warm water bath (55 °C). The resulting solution was sonicated prior to a 10 000 rpm centrifugation for 5 min in order to remove liposomes in the supernatant. Anionic nanoparticles in pellet form were suspended in 1 mL of DI water.

Preparation of Cisplatin Cationic Nanoparticles. Anionic nanoparticles in 1 mL of DI water were added to a dry positively charged nucleolipid (DOTAU) film for 2 h at 37 °C under stirring. A 10 000 rpm centrifugation (5 min) was performed to remove the supernatant. Cationic nanoparticles in pellet form were then diluted in 1 mL of DI water.

Preparation of Labeled Nanoparticles. A 0.05 mol % amount of DOPE-rhodamine or DOPE-fluorescein was added in dry anionic or cationic lipids used for nanoparticle preparation. Typically, stock solutions of positively charged nucleolipid (DOTAU) (10 mg/mL in dichloromethane) and DOPE-rhodamine (1 mg/mL in dichloromethane) were mixed at a molar ratio of 99.95/0.05 and placed in glass tubes. The mixture was dried under dry N_2 and then desiccated under vacuum overnight. This labeled dry lipid film was used to prepare cationic nanoparticles.

Preparation of Transplatin Nanoparticles. The nanoparticles were prepared following the same protocol described above except that the 5 mM cisplatin solution was replaced by a 1 mM transplatin solution (less soluble in water) and a 1 mM cisplatin solution.

Concentration Measurement. Nanoparticles (50 μL) were dessoluted in 5 mL of DI water with nitric acid (1%). After incubation overnight at room temperature, cisplatin concentration was evaluated with inductively coupled plasma atomic emission spectroscopy (ICP-AES) using a cisplatin range from 0.2 to 1 mg/L.

Transmission Electronic Microscopy (TEM). Nanoparticles were visualized by negative staining microscopy. Ten microliters of nanoparticles (1 mM) was transferred to a carbon-coated copper grid for 10 min. The sample was then dried and stained with 2.5% (w/w) of uranyl acetate in water for 5 min. The specimens were observed with a Hitachi H 7650 electron microscope.

Particle Size and Zeta Determination. Particle zeta and size were determined using a Zetasizer 3000 HAS MALVERN. Experiments were realized with 50 μL of the nanoparticles diluted in 1.2 mL of DI water, and measurements were performed at 25 °C.

Cisplatin Release Study. Eight tubes containing 150 μL of nanoparticles described above were incubated at 37 °C under a 300 rpm stirring. For different times (0, 1, 2, 3, 4, 5, 7, 10, 24 h), the corresponding sample was centrifugated (14 000 rpm) for 10 min, and cisplatin released was measured in the supernatant.

Cisplatin Release in Fetal Bovine Serum (FBS) Study. Twenty microliters of the nanoparticle solution described above and 130 μL of FBS were mixed and incubated at 37 °C under a 300 rpm stirring. For each time (0, 1, 2, 3, 4, 5, 7, 10, 24 h), the corresponding tube was centrifugated (14 000 rpm) for 10 min, and cisplatin released was measured in the supernatant.

Cytotoxicity Analysis. Cytotoxicity was assessed with formazan-based proliferation assay (CellTiter 96 Aqueous One Solution Cell Proliferation Assay kit, Promega). Human ovarian carcinoma cell line, A2780 (Oncodesign Biotechnology company, Dijon, France), A2780/Cis, has been developed by chronic exposure of parent cisplatin-sensitive A2780 (Oncodesign Biotechnology Company, Dijon, France); human ovarian cancer cell line, IGROV-1, was established at the Institut Gustave Roussy from a biopsy specimen of a woman with an ovarian cancer (Oncodesign Biotechnology Company, Dijon, France). IGROV-1/Cis was established by cultivating the IGROV-1 parental cell line with cisplatin, resulting in a cisplatin-resistant cell line (Oncodesign Biotechnology Company, Dijon, France). Mouse lymphocytic leukemia cell line, L1210, was established from a tumor developed following skin paintings with 0.2% methylcholanthrene in ether in a female BDA strain mouse (Oncodesign Biotechnology Company, Dijon, France). L1210/Cis was established *in vivo*, and cells were first propagated by heterotransplantation into BDA/2 mice treated with cisplatin at 5 mg/kg IP at day 4 and were adapted to *in vitro* suspension culture (Oncodesign Biotechnology Company, Dijon, France). Human adenocarcinoma epithelial tumor cell line, NIH:OVCAR-3, was established in 1982 by Hamilton *et al.* from the malignant ascites of a patient with progressive adenocarcinoma of the ovary (Oncodesign Biotechnology Company, Dijon, France). Mouse lymphoma cell line, P388, is a DBA/2 mouse lymphoma (Oncodesign Biotechnology Company, Dijon, France). Human ovarian carcinoma cell line, SKOV-3, and human glioblastoma cell line, U87, were purchased from American type Culture Collection/ATCC (Manassas, VA). Cells lines were incubated in Roswell Park Memorial Institute medium (RPMI, invitrogen), supplemented with 10% fetal bovine serum (FBS, invitrogen), 1% of non-essential amino acids, and 1% of L-glutamine at 37 °C in a 5% CO_2 atmosphere. Cells were split every 3−4 days to maintain monolayer coverage. Cells were seeded in each well of a 96-well plate (2500 cells/well) and allowed to attach overnight. Just before treatment, the medium was replaced by medium without serum (100 μL). The cells were incubated with concentration ranges of 500, 250, 100, 10, 1, 0.1, 0.01, and 0.001 μM of nanoparticles for the defined time. After treatment, cells were washed twice with PBS and incubated in 100 μL of medium with serum. Three days after, 20 μL of the MTS substrate was added to each well, and the plates were incubated for 2−4 h at 37 °C in 5% CO_2 incubator. Cell death was performed using a multiwell plate reader at 490 nm.

***In Vivo* Study.** Nanoparticles and free cisplatin were injected intravenously in rats (with a dose of 3, 5, 7, 9, 11 mg/kg and 3, 5, 7 mg/kg, respectively). Rat weights were followed for two months.

DNA Extraction and Gel Analysis. Cells were seeded in 10 cm Petri dishes (2×10^6 cells) for 24 h. The medium containing serum was removed from the well plates, replaced with 5 mL of the medium without serum, then treated with 5 μM of nanoparticles for 2 h. After being rinsed with PBS, cells were incubated in medium containing serum (10 mL) for 4 days. After a 4 days incubation time, all cells were collected, centrifugated for 10 min at 1000 rpm, and washed twice with PBS. DNA extraction was performed as per the manufacturer's instruction (GenElute plasmid miniprep Kit, Sigma-Aldrich) and analyzed by agarose gel electrophoresis.

Electrophoresis Studies. Electrophoresis studies were conducted on 0.8% agarose gels containing ethidium bromide in 0.5 Tris-borate-EDTA. For this purpose, 20 mL (250 ng/mL DNA concentration) of each sample was mixed with 4 mL of loading buffer (glycerol 30% (v/v), bromophenol blue 0.25% (w/v), and xylene cyanol 0.25 (w/v)) and subjected to agarose gel electrophoresis for 35 min at 100 mV. The electrophoresis gel was analyzed using a G.BOX camera.

Emergence of Resistant Cells Study. Cells were seeded in 12-well plates (10×10^3 cells/well) for 24 h. The medium containing serum was removed and replaced by 500 μL of the medium without serum and treated with a 5 μM solution of nanoparticles for 2 h. After being washed with PBS, cells were incubated in medium containing serum (1 mL). Cells viability analysis was carried out every 4 days over a period of 24 days. The cell culture medium was removed every 4 days. Cells were washed twice with PBS and were fixed in 250 μL of 100% ethanol for 15 min. At the end of the incubation period, cells were washed twice with PBS and were stained with 250 μL of crystal violet at 1% in water for 5 min at room temperature. The crystal violet excess was discarded by washing with DI water (1 mL, 2 times). One milliliter of a 33% acetic acid solution in water was added to solubilize the crystal violet, and the absorbance was recorded at 495 nm using a multiwell plate reader.

Confocal Fluorescence Microscopy. Two thousand cells/well were seeded overnight in an 8-well glass slide (Lab-Tek II, 154534) in the presence of 300 μL of culture medium. The medium was removed and replaced with 200 μL of medium without serum. The cells were incubated with labeled nanoparticles (50 μM) for 2 h. After incubation, cells were first washed with PBS, then fixed with 50 μL of Cytofix/Cytoperm buffer (BD bioscience) for 30 min on the slide and subsequently stained with 50 μL of diluted Hoechst 33334 (1 μg/mL, Invitrogen). Cells were washed twice with PBS and were finally mounted with a glass slide by using Invitrogen medium. Images were collected by using a confocal microscopy (Nikon C1 microscope).

Intracell Cisplatin Accumulation. Cells were seeded in 10 cm Petri dishes (2×10^6 cells) overnight. The medium was replaced with 5 mL of the medium without serum, and cells were treated with a 50 μM solution of nanoparticles (NP−, PS, NP+) and free cisplatin for 2, 4, and 6 h. After being washed with PBS, cells were harvested and 2×10^6 were lysed and diluted in 5 mL of DI water with 1% nitric acid. After incubation overnight at room temperature, cisplatin concentration was measured with inductively coupled plasma atomic emission spectroscopy (ICP-AES).

Flow Cytometry Study. IGROV-1 and SKOV-3 cell lines were seeded in 24-well plates (25×10^3 cells/well) overnight. The medium was replaced with 500 μL of the medium without serum. Cells were assayed for fluorescence intensity 2 h after being exposed to labeled nanoparticles (100 μM). After this treatment, cells were washed with PBS, treated with 100 μL of trypsine EDTA (invitrogen), and incubated for 5 min (37 °C) in a 5% CO_2 incubator. The cell suspension was then diluted to 200 μL using PBS and analyzed for fluorescence intensity using a FACS Canto dual laser flow cytometer.

Acknowledgment. This work has been supported by the French National Agency (ANR) in the frame of its programme EmergenceBio (project NANOVA, No. ANR-08-EBIO-013-01). The authors thank the SERCOMI Centre and the Laboratoire d'Hydrologie−Environnement, University of Bordeaux for technical assistance during TEM observations and ICP-AES measurements, respectively. P.B. acknowledges financial support from the Army Research Office. The authors report no conflict of interest.

Supporting Information Available: Details of all experiments, including size, zeta-potentials, infrared spectra, XPS analysis, stability, IC_{50}, mice and rat weight variation, DNA analysis, cells regrowths, uptake of cisplatin, FACS analysis, confocal and epifluorescence imaging. This material is available free of charge *via* the Internet at http://pubs.acs.org.

REFERENCES AND NOTES

1. Rosenberg, B.; VanCamp, L.; Trosko, J. E.; Mansour, V. H. Platinum Compounds: A New Class of Potent Antitumour Agents. *Nature* **1969**, *222*, 385–386.
2. Jamieson, E. R.; Lippard, S. J. Structure, Recognition, and Processing of Cisplatin−DNA Adducts. *Chem. Rev.* **1999**, *99*, 2467–2498.
3. Galanski, M.; Jakupec, M. A.; Keppler, B. K. Update of the Preclinical Situation of Anticancer Platinum Complexes: Novel Design Strategies and Innovative Analytical Approaches. *Curr. Med. Chem.* **2005**, *12*, 2075–2094.
4. Stordal, B.; Davey, M. Understanding Cisplatin Resistance Using Cellular Models. *IUBMB Life* **2007**, *59*, 696–699.
5. Yao, X.; Panichpisal, K.; Kurtzman, N.; Nugent, K. Cisplatin Nephrotoxicity: A Review. *Am. J. Med. Sci.* **2007**, *334*, 115–124.
6. Van den Bent, M. J.; van Putten, W. L. J.; Hilkens, P. H. E.; de Wit, R.; Van der Burg, M. E. L. Retreatment with Dose-Dense Weekly Cisplatin after Previous Cisplatin Chemotherapy Is Not Complicated by Significant Neuro-toxicity. *Eur. J. Cancer* **2002**, *38*, 387–391.
7. Duncan, R. Polymer Conjugates as Anticancer Nanomedicines. *Nat. Rev. Cancer* **2006**, *6*, 688–701.
8. Wagner, V.; Dullaart, A.; Bock, A. K.; Zweck, A. The Emerging Nanomedicine Landscape. *Nat. Biotechnol.* **2006**, *24*, 1211–1217.
9. Ferrari, M. Cancer Nanotechnology: Opportunities and Challenges. *Nat. Rev. Cancer* **2005**, *5*, 161–171.
10. Brigger, I.; Dubernet, C.; Couvreur, P. Nanoparticles in Cancer Therapy and Diagnosis. *Adv. Drug Delivery Rev.* **2002**, *54*, 631–651.
11. Peer, D.; Karp, J. M.; Hong, S.; Farokhzad, O. C.; Margalit, R.; Langer, R. Nanocarriers as an Emerging Platform for Cancer Therapy. *Nat. Nanotechnol.* **2007**, *2*, 751–760.
12. Boulikas, T. Low Toxicity and Anticancer Activity of a Novel Liposomal Cisplatin (Lipoplatin) in Mouse Xenografts. *Oncol. Rep.* **2004**, *12*, 3–12.
13. Burger, K. N. J.; Staffhorst, R. W. H. M.; de Vijlder, H. C.; Velinova, M. J.; Bomans, P. H.; Frederik, P. M.; de Kruijff, B. Nanocapsules: Lipid-Coated Aggregates of Cisplatin with High Cytotoxicity. *Nat. Med.* **2002**, *8*, 81–84.
14. Uchino, H.; Matsumura, Y.; Negjshj, T.; Koizumi, F.; Hayashi, T.; Honda, T.; Nishivama, N.; Kataoka, K.; Naito, S.; Kakizoe, T. Cisplatin-Incorporating Polymeric Micelles (NC-6004) Can Reduce Nephrotoxicity and Neurotoxicity of Cisplatin in Rats. *Br. J. Cancer* **2005**, *93*, 678–687.
15. Santosh, A.; Che-Ming, J. H.; Liangfang, Z. Polymer−Cisplatin Conjugate Nanoparticles for Acid-Responsive Drug Delivery. *ACS Nano* **2010**, *4*, 251–258.
16. Tian, Y.; Bromberg, L.; Lin, S. N.; Alan Hatton, T.; Tam, K. C. Complexation and Release of Doxorubicin from Its Complexes with Pluronic P85-*b*-Poly(acrylic acid) Block Copolymers. *J. Controlled Release* **2007**, *121*, 137–145.
17. Kaida, S.; Cabral, H.; Kumagai, M.; Kishimura, A.; Terada, Y.; Sekino, M.; Aoki, I.; Nishiyama, N.; Tani, T.; Kataoka, K. Visible Drug Delivery by Supramolecular Nanocarriers Directing to Single-Platformed Diagnosis and Therapy of Pancreatic Tumor Model. *Cancer Res.* **2010**, *70*, 7031–7041.
18. Boulikas, T.; Vougiouka, M. Recent Clinical Trials Using Cisplatin, Carboplatin and Their Combination Chemotherapy Drugs (Review). *Oncol. Rep.* **2004**, *11*, 559–595.
19. Dhar, S.; Gu, F. X.; Langer, R.; Farokhzad, O. C.; Lippard, S. J. Targeted Delivery of Cisplatin to Prostate Cancer Cells by Aptamer Functionalized Pt(IV) Prodrug-PLGA-PEG

Nanoparticles. *Proc. Natl. Acad. Sci. U.S.A.* **2008**, *105*, 17356–17361.
20. Dhar, S.; Kolishetti, N.; Lippard, S. J.; Farokhzad, O. C. Targeted Delivery of a Cisplatin Prodrug for Safer and More Effective Prostate Cancer Therapy *in Vivo*. *Proc. Natl. Acad. Sci. U.S.A.* **2011**, *108*, 1850–1855.
21. Paraskar, A. S.; Soni, S.; Chin, K. T.; Chaudhuri, P.; Muto, K. W.; Berkowitz, J.; Handlogten, M. W.; Alves, N. J.; Bilgicer, B.; Dinulescu, D. M.; *et al.* Harnessing Structure–Activity Relationship To Engineer a Cisplatin Nanoparticle for Enhanced Antitumor Efficacy. *Proc. Natl. Acad. Sci. U.S.A.* **2010**, *107*, 12435–12440.
22. Gissot, A.; Camplo, M.; Grinstaff, M. W.; Barthélémy, P. Nucleoside, Nucleotide and Oligonucleotide Based Amphiphiles: A Successful Marriage of Nucleic Acids with Lipids. *Org. Biomol. Chem.* **2008**, *6*, 1324–1333.
23. Barthélémy, P. Nucleoside-Based Lipids at Work: From Supramolecular Assemblies to Biological Applications. *CR Chimie* **2009**, *12*, 171–179.
24. Khiati, S.; Pierre, N.; Andriamanarivo, S.; Grinstaff, M. W.; Arazam, N.; Nallet, F.; Navailles, L.; Barthélémy, P. Anionic Nucleotide-Lipids for *In Vitro* DNA Transfection. *Bioconjugate Chem.* **2009**, *20*, 1765–1772.
25. Chabaud, P.; Camplo, M.; Payet, D.; Serin, G.; Moreau, L.; Barthélémy, P.; Grinstaff, M. W. Cationic Nucleoside Lipids for Gene Delivery. *Bioconjugate Chem.* **2006**, *17*, 466–472.
26. Burger, K. N.; Staffhorst, R. W.; De Vijlder, H. C.; Velinova, M. J.; Bomans, P. H.; Frederik, P. M.; Kruijff, B. Nanocapsules: Lipid-Coated Aggregates of Cisplatin with High Cytotoxicity. *Nat. Med.* **2002**, *8*, 81–84.
27. Legendre, F.; Véronique Bas, V.; Kozelka, J.; Chottard, J. C. A Complete Kinetic Study of GG *versus* AG Platination Suggests that the Doubly Aquated Derivatives of Cisplatin Are the Actual DNA Binding Species. *Chem.—Eur. J.* **2000**, *6*, 2002–2010.
28. Chupin, V.; de Kroon, A. I.; de Kruijff, B. Molecular Architecture of Nanocapsules, Bilayer-Enclosed Solid Particles of Cisplatin. *J. Am. Chem. Soc.* **2004**, *42*, 13816–13821.
29. Zwelling, L. A.; Kohn, K. W.; Ross, W. E.; Ewig, R. A.; Anderson, T. Kinetics of Formation and Disappearance of a DNA Cross-Linking Effect in Mouse Leukemia L1210 Cells Treated with *cis* and *trans*-Diamminedichloroplatinum(II). *Cancer Res.* **1978**, *38*, 1762–1768.
30. Kelland, L. The Resurgence of Platinum-Based Cancer Chemotherapy. *Nat. Rev. Cancer* **2007**, *7*, 573–584.
31. Kartalou, M.; Essigmann, J. M. Mechanisms of Resistance to Cisplatin. *Mutat. Res.* **2001**, *478*, 23–43.
32. Siddik, Z. H. Cisplatin: Mode of Cytotoxic Action and Molecular Basis of Resistance. *Oncogene* **2003**, *22*, 7265–7279.